

# Fragmentation of $Xe^{129}$ in the Liquid-Gas Phase Transition Region

Mehmet ERDOĞAN, Nihal BÜYÜKÇİZMECİ, Rıza OĞUL  
*Department of Physics, University of Selçuk, 42075 Konya-TURKEY*  
*e-mail: nihal@selcuk.edu.tr*

Received 15.03.2007

We analyzed the fragmentation of the  $Xe^{129}$  nucleus to determine the effects of surface and symmetry energies on the fragment distribution on the basis of the statistical multifragmentation model. Relative yields of fragments were classified with respect to the mass number of the fragments in the transition region. It was found that the symmetry energy of the hot fragments produced in the statistical freeze-out is very important for isotope distributions. However, its influence on the mean fragment mass distributions is negligible. On the other hand, it was demonstrated that surface energy significantly influences the fragment distribution while the symmetry energy contribution remains negligible.

**Key Words:** Nuclear multifragmentation, mass distribution, symmetry energy, surface energy, excitation energy.

## Introduction

Multifragmentation of nuclei is a promising process for studying nuclear matter properties at the extreme conditions of high excitations energies, subsaturation densities, and at different isospins. We expect to establish its connection to a nuclear liquid-gas phase transition. Recently, we carried out some calculations on nuclear multifragmentation that point out some signals of a liquid gas type phase transitions in nuclear collisions.<sup>1-5</sup> Like other complicated many-body processes, this phenomenon can be successfully treated within the statistical framework. This process is mainly associated with abundant production of intermediate mass fragments (IMFs, with mass  $A \approx 5-40$ ). However, at the onset of multifragmentation, heavy residues are also produced, which have previously been associated only with the compound nucleus. At very high excitation energies ( $E^* > 2-3$  MeV/nucleon), IMF production gives way to the total vaporization of nuclei into a nucleus and very light clusters. In recent years, the fragmentation event was previously studied in excited nuclear matter by considering the liquid-gas phase transition and it has been shown that heated nuclear matter has characteristic van der Waals behavior.<sup>6-10</sup>

## Nuclear Fragmentation

Statistical models are used in situations when an equilibrated source can be defined in the nuclear reaction. The most famous example of such a source is the compound nucleus introduced by Niels Bohr in 1936. The standard compound nucleus picture is valid only at low excitation energies when sequential evaporation of light particles and fission are the dominating decay channels. However, this concept cannot be directly applied at high excitation energies ( $E^* \geq 2\text{-}3$  MeV/nucleon), when the nucleus rapidly disintegrates into many fragments. As was shown in many experiments, an equilibrated source can be formed in this case as well, and statistical models are generally very successful in describing the fragment production.<sup>11–15</sup>

We carried out our calculations on the basis of the statistical multifragmentation model (SMM).<sup>8</sup> The model is based upon the assumption of statistical equilibrium at a low-density freeze-out state. According to the SMM, we assume all breakup channels (partitions) are composed of nucleons. However, the model assumes a microcanonical ensemble of breakup channels and the system should obey the laws of conservation of energy  $E^*$ , mass number  $A$ , and charge number  $Z$ . In the microcanonical treatment the statistical weight of breakup channel is

$$W_j \propto \exp(S_j(E^*, A, Z)) \quad (1)$$

where  $S_j$  is the entropy of the system in channel  $j$ . The decay channels are generated by the Monte Carlo method according to their statistical weights.

Light fragments with mass number  $A \leq 4$  are considered elementary particles (nuclear gas) having only translational degrees of freedom. The fragments with mass number  $A > 4$  are treated as heated nuclear liquid drops. In this way, one may study the nuclear liquid-gas coexistence in the freeze-out volume. Free energies,  $F_{AZ}$ , of each fragment are parameterized as a sum of the bulk, surface, Coulomb, and symmetry energy contributions

$$F_{AZ} = F_{AZ}^{Bulk} + F_{AZ}^{Surface} + F_{AZ}^{Symmetry} + F_{AZ}^{Coulomb} \quad (2)$$

The bulk contribution is given as

$$F_{AZ}^{bulk}(T) = -(W_0 + T^2/\varepsilon_0)A \quad (3)$$

where  $T$  is the temperature, the parameter  $\varepsilon_0$  is related to the level density, and  $W_0 = 16$  MeV is the binding energy of infinite nuclear matter. Contribution of the surface energy is given by

$$F_{AZ}^{Surface}(T) = B_0 \left( \frac{T_c^2 - T^2}{T_c^2 + T^2} \right)^{5/4} A^{2/3} \quad (4)$$

where  $B_0 = 18$  MeV is the surface coefficient and  $T_c = 18$  MeV is the critical temperature of the infinite nuclear matter. Contribution of the Coulomb energy is given by

$$E_{AZ}^C = c \frac{Z^2}{A^{1/3}} \quad (5)$$

where  $c$  is the Coulomb parameter. In the Wigner-Seitz approximation, the parameter is obtained as

$$c = \left( \frac{3}{5} \right) \left( \frac{e^2}{r_0} \right) \left[ 1 - \left( \frac{\rho}{\rho_0} \right)^{1/3} \right] \quad (6)$$

where  $e$  is the charge unit,  $r_0 = 1.17 \text{ fm}$ , and  $\rho_0$  is the normal nuclear matter density ( $0.15 \text{ fm}^{-3}$ ). Finally, the symmetry energy is given by

$$E_{AZ}^{\text{symmetry}} = \gamma(A - 2Z)^2/A \quad (7)$$

where  $\gamma = 25 \text{ MeV}$  is the symmetry energy parameter. All of the parameters given above are taken from the Bethe-Weizsacker formula and correspond to the assumption of isolated fragments with normal density in the freeze-out configuration.

The surface term is a function of 2 parameters, which are the coefficient  $B_0$  and the critical temperature  $T_c$ . The critical temperature for the nuclear liquid-gas phase transition in infinite matter is previously defined as  $18 \text{ MeV}$ , but this temperature is different from the phase transition temperature in finite hot nuclei, which are essentially lower, around  $5\text{-}6 \text{ MeV}$ .  $T_c$  should be considered a model parameter characterizing the temperature dependence of the surface tension in finite nuclei. This T-dependence leads to a correct surface contribution to the level densities of nuclei at low temperatures. The relation is previously studied between the surface energy and  $T/T_c$ .<sup>4</sup> The decrease in the surface energy with increasing  $T/T_c$  (see formula 4) influences the fragment production. The surface parameter may change at low density in surroundings consisting of nucleons and hot fragments. In this study, we studied the influence of the surface and symmetry energy in nuclear fragmentation.

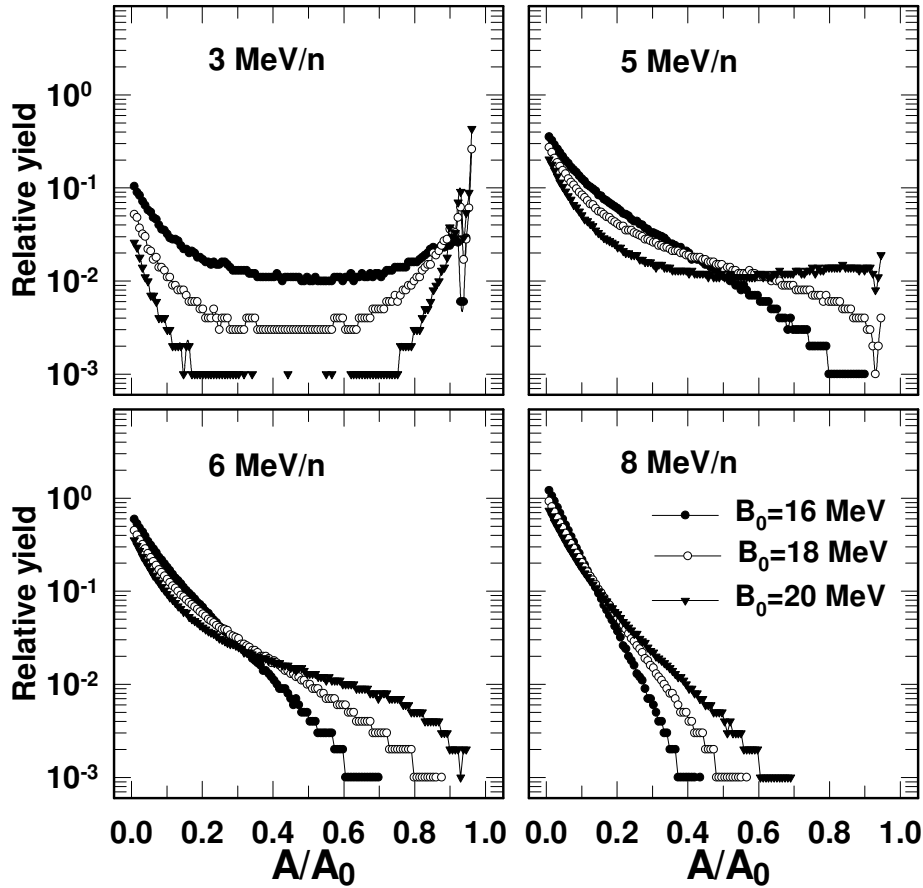
The surface energy is quite important, because the surface contribution to the total energy of the system increases due to the production of new fragments. Hence, small changes in the value of the surface energy produce significant changes in the fragment mass and charge distributions. This concept is demonstrated in Figure 1 for different excitation energies for Xe<sup>129</sup> sources with a freeze-out density  $\rho = \rho_0/3$ . The influence of the symmetry energy was also studied in the freeze-out volume at excitation energy of  $5 \text{ MeV/nucleon}$ . The symmetry energy coefficient  $\gamma$  was chosen as  $8, 14,$  and  $25 \text{ MeV}$ .

To characterize the mass distributions we use the  $A^{-\tau}$  fit of the fragment yields in the nuclear fragmentation.<sup>4,16,17</sup> Here,  $\tau$  is the critical exponent (for mass distribution). In all calculations, the mass distribution of IMFs is considered in the range  $6 \leq A \leq 40$ . The lighter fragments are considered a nuclear gas.

## Results and Discussion

We obtained almost the same results as Botvina et al.<sup>1</sup> Figure 1 shows the relative yield of hot primary fragments versus  $A/A_0$  for Xe<sup>129</sup> at different excitation energies  $3, 5, 6,$  and  $8 \text{ MeV/nucleon}$  for the surface energies  $16, 18,$  and  $20 \text{ MeV}$ . We observed that the relative yield of hot fragments produced a U-shape distribution for  $T \leq 5 \text{ MeV}$ . This situation corresponds to the partitions with a few small fragments and a large residual fragment. At high excitation energies ( $T \geq 6 \text{ MeV}$ ), the large fragments disappear, and an exponential-like fall-off is observed. However, the number of relative yield of hot fragments increases at small  $B_0$  values. As can be seen from Figure 1, the transition region is observed between these temperature values.

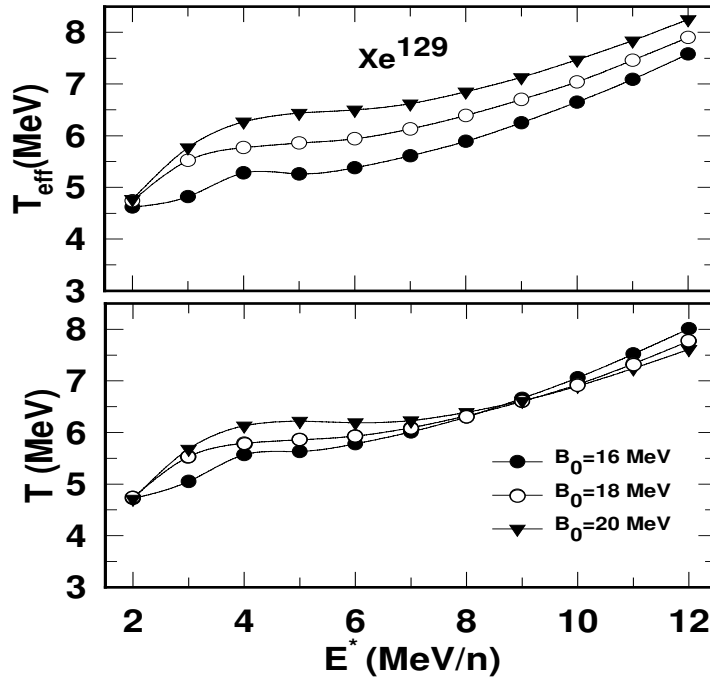
We show that the symmetry energy effect on isotope distribution can survive after secondary deexcitation. For this reason, an extraction of this symmetry energy from the data is important not only for the context of nuclear physics but also for nuclear astrophysical studies.<sup>3</sup>



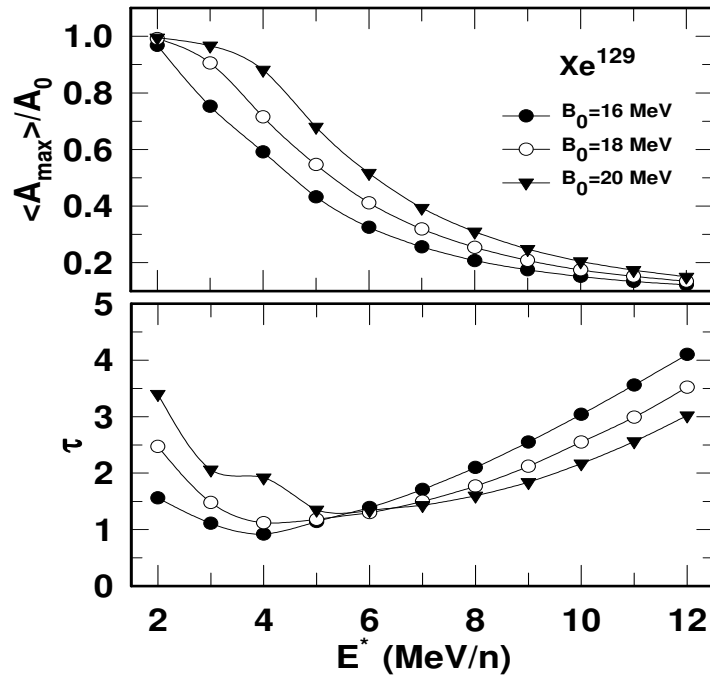
**Figure 1.** Relative yield of hot primary fragments versus  $A/A_0$  for  $\text{Xe}^{129}$  for different surface energy coefficients  $B_0 = 16, 18, \text{ and } 20$  MeV at different excitation energies 3, 5, 6, and 8 MeV/nucleon.

Figure 2 shows the effects of the coefficient  $B_0$  on the caloric curve for  $\text{Xe}^{129}$  nucleus at 2 different temperatures. Effective temperature  $T_{eff}$  is found from the energy balance in the freeze-out volume by assuming that the properties of fragments are the same as those of isolated nuclei. The other one is the freeze-out temperature  $T$  that is included in medium modifications of the fragment properties at different  $B_0$ . The variations in effective and freeze-out temperatures with  $E^*$  are presented in Figure 2. This concept was previously studied for the nucleus of  $\text{Au}^{197}$  and the connection of these temperatures was shown for  $\text{Au}^{197}$  with respect to the excitation energies for different  $B_0$  coefficients.<sup>3</sup> A lower effective temperature is clearly seen at smaller  $B_0$  values. Nevertheless, we can see that the system disintegrates into lighter fragments, and  $A_{max}$  becomes smaller (top panel of Figure 3). At low excitation energies, the behavior of both temperatures is similar but for very high excitation energies as the system disintegrates only into light IMFs the freeze-out temperature is higher at smaller  $B_0$ .

In multifragmentation, the mass number of the largest fragment  $A_{max}$  and  $\tau$  parameter as a function of the excitation energy are presented at different surface energies in the bottom panel in Figure 3. Here, we see that the maximum variance values for  $\text{Xe}^{129}$  source are at excitation energy of 4-5 MeV/nucleon, which corresponds to the transition region.  $\tau$  parameter shows a general trend in the variation of the mass distributions and it depends strongly on the excitation energy for different  $B_0$  coefficients (bottom panel in Figure 3). The same trend can be seen for the nucleus of  $\text{Au}^{197}$  in the freeze-out volume.<sup>3</sup>



**Figure 2.** SMM calculations of characteristics of hot fragments from Xe sources for different surface energy coefficients  $B_0 = 16, 18,$  and  $20$  MeV as a function of the excitation energy  $E^*$ . Top panel: effective temperature  $T_{\text{eff}}$ ; bottom panel: freeze-out temperature.



**Figure 3.** SMM calculations of characteristics of hot fragments from Xe sources for different surface energy coefficients  $B_0 = 16, 18,$  and  $20$  MeV as a function of the excitation energy  $E^*$ . Top panel: reduced mass number of the largest fragment  $A_{\text{max}}/A_0$ ; bottom panel:  $\tau$  parameter.

The influence of the symmetry energy was not seen on yields of hot fragments in the freeze-out volume. As can be seen in Figure 4, modifications of symmetry energy by means of  $\gamma$  do not influence the yields of hot fragments.

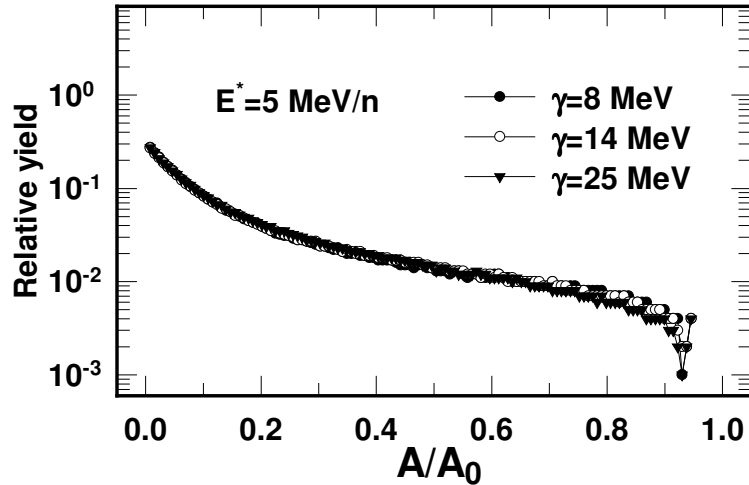


**Figure 4.** Influence of the symmetry energy coefficient  $\gamma$  on yields of hot fragments in the freeze-out volume.

## Acknowledgement

The authors thank A.S. Botvina for many helpful discussions.

## References

1. A.S. Botvina, N. Buyukcizmeci, M. Erdogan, J. Lukasik, I.N. Mishustin, R. Ogul and W. Trautmann, **Phys. Rev. C** **74**, 044609 1-10 (2006).
2. N. Buyukcizmeci, R. Ogul and A.S. Botvina, **Eur. Phys. J. A** **25**, 57 (2005).
3. R. Ogul, N. Buyukcizmeci and A.S. Botvina, **Nucl. Phys. A** **749**, 126 (2005).
4. R. Ogul and A.S. Botvina, **Phys. Rev. C** **66**, 051601 (2002).
5. R. Ogul and U. Atav, **Physica Scripta** **67**, 34 (2003).
6. L.G. Moretto and G.J. Wozniak, **Ann. Rev. Nucl. Part. Sci.** **43**, 379 (1993).
7. A.S. Botvina and I.N. Mishustin, **Phys. Rev. C** **63**, 061601 (2001).
8. J.P. Bondorf, A.S. Botvina, A.S. Iljinov, I.N. Mishustin and K. Sneppen, **Phys. Rep.** **257**, 133 (1995).
9. D.H.E. Gross, **Phys. Rep.** **279**, 119 (1997).
10. M. D'Agostino, A.S. Botvina, P.M. Milazzo, M. Bruno, G.J. Kunde, D.R. Bowman, L. Celano, N. Colonna, J.D. Dinius, A. Ferrero, M.L. Fiandri, C.K. Gelbke, T. Glasmacher, F. Gramegna, D.O. Handzy, D. Horn, W.C. Hsi, M. Huang, I. Iori, M.A. Lisa, W.G. Lynch, L. Manduci, G.V. Margagliotti, P.F. Mastinu, I.N. Mishustin, C.P. Montoya, A. Moroni, G.F. Peaslee, F. Petruzzelli, L. Phair, R. Rui, C. Schwarz, M.B. Tsang, G. Vannini and C. Williams, **Phys. Lett. B** **371**, 175 (1996).

11. A.S. Botvina, I.N. Mishustin, M. Begemann-Blaich, J. Hubele, G. Imme, I. Iori, P. Kreutz, G.J. Kunde, W.D. Kunze, V. Lindenstruth, U. Lynen, A. Moroni, W.F.J. Muller, C.A. Ogilvie, J. Pochodzalla, G. Raciti, Th. Rubehn, H. Sann, A. Schuttauf, W. Seidel, W. Trautmann, A. Wornner, *Nucl. Phys. A* **584**, 737 (1995).
12. R.P. Scharenberg, B.K. Srivastava, S. Albergo, F. Bieser, F.P. Brady, Z. Caccia, D.A. Cebra, A.D. Chacon, J.L. Chance, Y. Choi, S. Costa, J.B. Elliott, M.L. Gilkes, J.A. Hauger, A.S. Hirsch, E.L. Hjort, A. Insolia, M. Justice, D. Keane, J.C. Kintner, V. Lindenstruth, M.A. Lisa, H.S. Matis, M. McMahan, C. McParland, W.F.J. Muller, D.L. Olson, M.D. Partlan, N.T. Porile, R. Potenza, G. Rai, J. Rasmussen, H.G. Ritter, J. Romanski, J.L. Romero, G.V. Russo, H. Sann, A. Scott, Y. Shao, T.J.M. Symons, M. Tincknell, C. Tuve, S. Wang, P. Warren, H.H. Wieman, T. Wienold and K. Wolf, **Phys. Rev. C** **64**, 054602 (2001).
13. L. Pienkowski, K. Kwiatkowski, T. Lefort, W.-C. Hsi, L. Beaulieu, V.E. Viola, A. Botvina, R.G. Korteling, R. Laforest, E. Martin, E. Ramakrishnan, D. Rowland, A. Ruangma, E. Winchester, S.J. Yennello, B. Back, H. Breuer, S. Gushue and L.P. Remsberg, **Phys. Rev. C** **65**, 064606 (2002).
14. N. Bellaize, O Lopez, J.P. Wieleczko, D. Cussol, G. Auger, C.O. Bacri, F. Bocage, B. Borderie, R. Bougault, B. Bouriquet, R. Brou, P. Buchet, A.M. Buta, J.L. Charvet, A. Chbihi, J. Colin, R. Dayras, N. De Cesare, A. Demeyer, D. Dore, D. Durand, J.D. Frankland, E. Galichet, E. Genouin-Duhamel, E. Gerlic, B. Guiot, D. Guinet, S. Hudan, G. Lanzalone, P. Lautesse, F. Lavaud, J.L. Laville, J.F. Lecolley, R. Legrain, N. Le Neindre, L. Manduci, J. Marie, L. Nalpas, J. Normand, M. Parlog, P. Pawlowski, E. Plagnol, M.F. Rivet, E. Rosato, R. Roy, F. Saint-Lauren, J.C. Steckmeyer, G. Tabacaru, B. Tamain, E. van Lauwe, L. Tassan-Got, E. Vient, M. Vigilante and C. Volant, **Nucl. Phys. A** **709**, 367 (2002).
15. S.P. Avdeyev, V.A. Karnaukhov, L.A. Petrov, V.K. Rodionov, P.A. Rukoyatkin, V.D. Toneev, H. Oeschler, O.V. Bochkarev, L.V. Chulkov, E.A. Kuzmin, A. Budzanowski, W. Karcz, M. Janicki, E. Norbeck, A.S. Botvina and K.K. Gudima, **Nucl. Phys. A** **709**, 392 (2002).
16. A.L. Goodman, J.I. Kapusta, and A.Z. Mekjian, *Phys. Rev. C* **30**, 851 (1984).
17. J. Hüfner, **Phys. Rep.** **125**, 129 (1985).